Development of Miniature Magnetometers

Dennis K. Wickenden, Thomas J. Kistenmacher, Robert Osiander, Scott A. Ecelberger, R. Ben Givens, and John C. Murphy

Some of the highlights of the ongoing program within the Sensor Science Group of APL's Milton S. Eisenhower Research and Technology Development Center to develop novel magnetometers are summarized. In particular, two approaches are described: a magnetostrictive device based on the deflection of a Terfenol-D coated single-crystal silicon cantilever and a Lorentz-force device based on a classical xylophone resonator. Both magnetometers, even though at early stages of development, are state of the art in terms of sensitivity and offer a number of advantages for field applications: small size, high sensitivity, integration on a silicon chip, and vector capability. Using standard microelectromechanical system (MEMS) machining techniques, both classes—together with others under consideration—can be fabricated into planar three-axis magnetometers and into one- or two-dimensional arrays for magnetic imaging applications.
(Keywords: Lorentz force, Magnetic field, Magnetometer, Magnetostriction, Resonator.)

INTRODUCTION

Today, interest is increasing in the development of miniature magnetometers for mapping magnetic fields in extraterrestrial, industrial, biomedical, oceanographic, and environmental applications. The many potential uses of such instruments, just within the Johns Hopkins community, include the following:

- Space physics—for the measurement of absolute field levels and curl of interplanetary space (using suitable arrays of sensors) and satellite-generated fields
- Oceanography—for the detection of ships, mineral deposits, and other magnetic objects
- Biomedicine—for the imaging of magnetic patterns, and, for example, tracking the location and orientation of instruments in microsurgery (the latter will be particularly helpful as the technology moves more to robotic or tele-operated systems)
- Environmental science—in the imaging or detection of magnetic fields on the Earth's surface or in the

atmosphere, for example, in the detection of pipeline corrosion
- Transportation—in the measurement of deflections in crash test experiments and as one of the many sensors in automatically piloted road vehicles

The trend in magnetometer design and development is constantly toward smaller size, lower power consumption, and lower cost for similar performance.[1] The need for significant improvements in sensitivity independent of size, power, and cost is also important but usually only in specialized applications. Toward the objectives of improved size, power, and cost, recent innovations have included the use of piezoresistive[2] cantilevers and magnetometers based on electron-tunneling effects.[3] The sensitivities of these magnetometers, defined as the minimum detectable field change, are generally in the range of 1 μT to 1 mT, corresponding to 10^{-2} to 10 Oe. In this article, we summarize some of the highlights of the ongoing program within the Sensor Science Group of APL's Milton S. Eisenhower Research and Technology Development Center to develop novel magnetometers capable of meeting most, if not all, of the potential applications previously outlined. In particular, we describe two approaches: a magnetostrictive device based on the deflection of a Terfenol-D coated single-crystal silicon cantilever and a Lorentz-force device based on a classical xylophone resonator.

MAGNETOSTRICTIVE MAGNETOMETER

When a polycrystalline ferromagnetic sample is placed in a magnetic field, it either elongates or contracts along the field direction and does the opposite in the transverse direction, to maintain an almost constant volume. Such changes in dimension, below the Curie temperature, are caused by rotation of the magnetic domains in the material and are called magnetostriction. For most ferromagnetic materials, including nickel and iron, the magnetostriction coefficients are quite small and range from ±10 to 100 ppm in fields on the order of 0.5 T. However, giant magnetostriction, with magnetostriction coefficients up to 0.2%, has been observed in numerous rare-earth/iron alloys, including Terfenol-D [$(Dy_{0.7}Te_{0.3})Fe_2$]. A number of applications for such alloys have been anticipated and include surface acoustic wave devices, actuators, and magnetic sensors. Whereas device applications are envisioned in bulk,[4-7] ribbon,[8] and thin-film[9,10] forms, the latter is advantageous for the production of miniaturized magnetometers for a variety of reasons. The shape of the magnetostriction/applied field curve is sigmoidal with very little magnetostriction at low fields. It tends to make such material unsuitable for low-field magnetometry. However, it has been shown that the shape of the curve depends on whether the sample is in tension or compression, and that, when in tension, a significant gradient exists at low fields.[11] To date, however, no values for the magnetostriction coefficient of Terfenol-D have been quoted for fields lower than 5 mT.

The Sensor Science Group has been developing novel sensors using surface micromachining of silicon with standard microelectromechanical system (MEMS) fabrication techniques.[12] In the simplest example of surface micromachining, a sacrificial layer of silicon dioxide is deposited or grown on a silicon substrate and patterned using photolithography for selective removal in regions where the mechanical structure is to be attached to the silicon structure. The layer for the mechanical structure (usually polysilicon) is then deposited and patterned. Finally, the sacrificial layer is etched away to release the polysilicon structure. More complex structures are fabricated using additional layers of materials having the desired properties. For example, most of the MEMS sensors we are currently developing are fabricated at the DARPA-supported Multi-User MEMS Processes (MUMPs) foundry at the Microelectronics Center of North Carolina (MCNC). This service uses three polysilicon and two silicon dioxide sacrificial layers of differing thicknesses deposited on a silicon nitride layer to electrically isolate the structures from the silicon substrate, which enables various structures to be processed, including cantilevers, diaphragms, and actuators.[12] Before final release at APL, various materials can be selectively deposited to produce specific sensor action. For example, for a magnetostrictive magnetometer, a thin film of Terfenol-D is deposited onto a MEMS cantilever. This film will naturally be placed under tension when it is deposited onto a silicon substrate because of the difference in coefficients of thermal expansion. When the completed device is placed in a magnetic field, the magnetostriction of the Terfenol-D causes the cantilever to deflect, similar to a bimetallic strip when subjected to heat. The deflection is a function of the magnetic field strength and can be measured using various transduction schemes, including either optical beam deflection or changes in capacitance. The latter is particularly appropriate to MUMPs devices, since the bottom polysilicon layer, used as one electrode of a parallel plate capacitor, is within a few micrometers of the cantilever, and sensibly sized capacitances can be obtained with relatively small areas. Furthermore, it is possible to incorporate various electronic circuits into the design, and the completed device will be only a few square millimeters in size.

Figure 1 is an illustration of an APL-designed and -fabricated magnetostrictive magnetometer.[13] The active transduction element is a commercial (001)-oriented single-crystal silicon cantilever, obtained from Digital Instruments, Inc., with dimensions on the order

of 450 μm (length) by 50 μm (width) and 1–3 μm (thickness). This cantilever, developed primarily for scanning tunneling and atomic force microscopy, was chosen because of its availability before MUMPs cantilevers could be designed and processed. The Terfenol-D film was deposited in a high-vacuum DC-magnetron sputtering system, which uses argon as plasma gas and a polycrystalline target obtained from Etrema Products, Inc. The film composition was determined by X-ray energy dispersive spectroscopy and shown to be very close to that of the Etrema target. The structural properties were ascertained from $\theta/2\theta$ X-ray diffraction data collected on a Phillips APD powder diffractometer using graphite-monochromatized CuKα radiation. The presence of only broadly diffuse maxima in the diffraction pattern suggested an amorphous film structure. This amorphous structure is particularly advantageous since it leads to a sharp increase in magnetostriction amplitude at low fields,[11] allows neglect of crystalline anisotropy, offers minimal hysteresis, and yields a room-temperature thermal expansion coefficient apparently near that of (001) silicon. The latter is important since residual strain caused by elevated temperature processing, together with a thermal expansion coefficient mismatch between the film and the cantilever, can lead to significant deformation of the cantilever on cooling to room temperature. Significant residual strain may also affect the temperature stability of working devices.

In operation, the cantilever is driven at its fundamental resonance frequency (typically at $f_0 \approx 10$ kHz) by coupling to a magnetic excitation field induced in coils wound around a Lexan spindle. These same Lexan forms house a second, parallel set of coils that serve as a DC field and bias supply, with an approximate field of 2 μT/mA. The Lexan cradle, with a core diameter of ≈2 cm and a coil separation of ≈1 cm, approximates a Helmholtz configuration and sets the size of the active magnetometer elements shown in Fig. 1.

The advantage of operating the device at resonance is that the displacement x of the resonator as a function of frequency f is proportional to

$$\frac{F}{k\sqrt{\left(1-\frac{f^2}{f_0^2}\right)^2+\left(\frac{1}{Q}\,\frac{f}{f_0}\right)^2}},$$

where F is the driving force, k is the restoring force, and the quality factor Q is a measure of the damping force. Thus, at resonance the displacement is increased by a factor of Q over a static system.

The field-induced deflection was sensed using the compact optical beam deflection technique depicted in Fig. 1. The output of a 5 mW, 660-nm laser diode, modulated at a frequency f_1 (typically 11 kHz), was

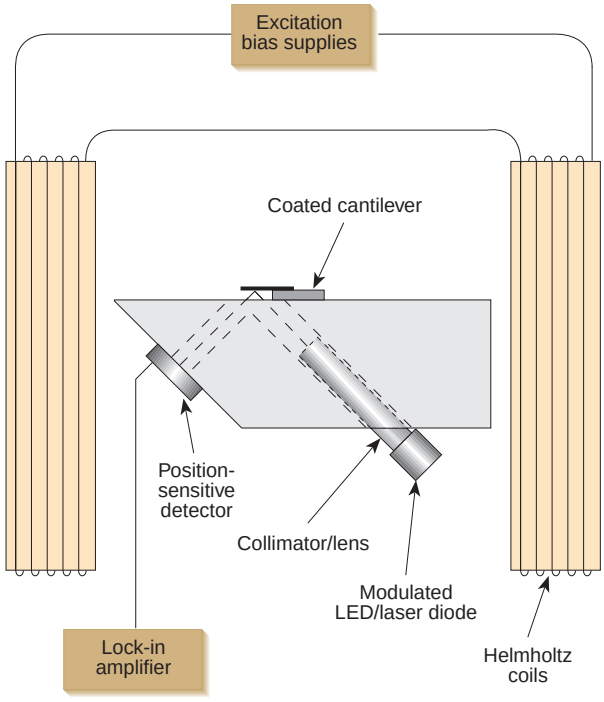

Figure 1. Cross section of the microelectromechanical-based magnetostrictive magnetometer. The separation between field coils is ≈1 cm. The light source is either a light-emitting diode (LED) or semiconductor laser.

coupled into a 62-μm-core-dia. multimode fiber-optic cable; the cleaved end of the cable was positioned close (≈100 μm) under the tip of the cantilever. The deflected beam was captured by a position-sensitive detector (PSD) whose output was monitored by a lock-in amplifier at the difference frequency $f_1 - f_0$. In a typical field detection protocol, the peak-to-peak amplitude of the AC excitation field was set to 50 μT, and the DC external field was cycled (±2-mT limits) over several full hysteresis loops ($M_s \approx 8.3$ kG; $H_c \approx 8.5$ Oe) and returned to zero. Subsequent ramping of the DC field from zero to a maximum of 200 mT (Fig. 2) yielded a

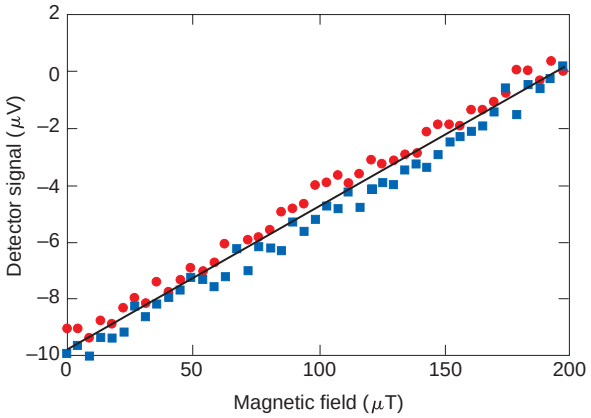

Figure 2. Response of the microelectromechanical-based magnetostrictive magnetometer to increasing (circles) and decreasing (squares) DC magnetic field.

linear dependence, with minimal hysteresis, of the output of the PSD on the magnitude of the external DC magnetic field. From the uncorrected experimental data displayed in Fig. 2, a resolution of ≈50 μV/mT and a sensitivity near 1 μT were deduced. Further optimization of the optical detection scheme should increase the sensitivity still further. In addition, data from numerous runs also suggest a very high mechanical and thermomagnetic stability for this magnetostrictive magnetometer.

These results represent state of the art for a MEMS-based magnetometer and, importantly, demonstrate for the first time that Terfenol-D has a measurable magnetostrictive coefficient at magnetic fields at the millitesla level. The recently reported piezoresistive device[2] consists of a single-crystal silicon cantilever, 200 mm long, onto the end of which is glued a small (700 ng) grain of magnetic material. Measurements performed either at low temperature (59.1 K) with a microcrystal of a high-critical-temperature superconductor or at room temperature with a small iron crystal gave sensitivities of 5 and 50 mT, respectively. The magnetometer based on electron tunneling is bulk-micromachined from silicon. It consists of a silicon substrate on which a fixed electron tunneling tip is etched and a deflection electrode is deposited, and is bonded to a low-stress silicon nitride membrane (2.5 × 2.5 mm). The deflection of the membrane is caused by the Lorentz force induced between the applied fields and the current flowing in a multiloop conductor deposited on top of the membrane. To date, it has been possible to produce only a single loop, resulting in a preliminary noise equivalent magnetic field of only 6 $\mu T\sqrt{Hz}$.[3]

LORENTZ-FORCE MAGNETOMETER

This magnetometer is a simple, small, lightweight, low-cost, and low-power-consumption sensor that uses the Lorentz force to measure vector magnetic fields.[14] The device, which is based on a classical xylophone resonator, is intrinsically linear and has a very wide dynamic range that can measure magnetic field strengths from nanoteslas to teslas.

Figure 3 shows a prototype magnetometer. It consists of a thin aluminum bar (type 2024-T3), 39.00 × 2.43 × 0.81 mm in dimensions, supported by two 18-mm-long strands of 3 × 0.08-mm-dia. tinned copper wires. The wires are bonded to the bar to provide low-resistance electrical contacts, and positioned at the nodal points expected for a bar free at both ends and vibrating in its fundamental mode.[15] In operation, alternating currents up to 1 A, generated by a sinusoidal source oscillating at the fundamental transverse resonant mode (f_0 = 2.79 kHz), are supplied to the bar, and the device is placed inside a set of 35-cm-dia. Helmholtz coils. The Lorentz force generated by the current and

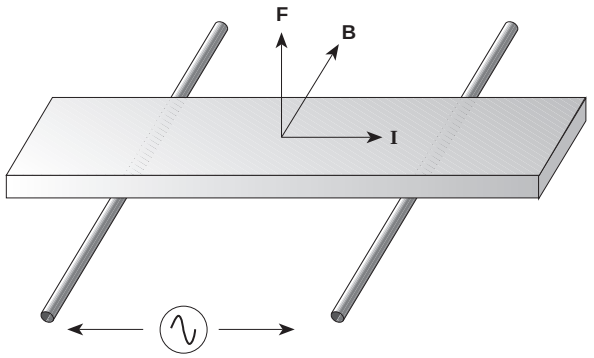

Figure 3. Diagram of the principle of operation of the xylophone magnetometer. **F** = Lorentz force, **I** = current, and **B** = applied magnetic field.

the applied magnetic field ($\mathbf{F} = \mathbf{I} \times \mathbf{B}$) caused the xylophone to vibrate in its fundamental mode, the amplitude being proportional to the vector component of the field in the plane of the bar and parallel to the support wires. This amplitude was measured using a bench-top optical beam deflection technique in which the deflection of a DC-driven diode laser beam was reflected from one of the free ends of the bar onto a PSD. The PSD used was a commercial quadcell wired up as a bicell; the difference in outputs was fed to a lock-in amplifier whose reference signal was obtained from the xylophone resonator drive waveform. A fluxgate magnetometer, with a quoted field measurement range of ± 0.1 mT and a noise figure of <15 pT rms $\sqrt{Hz}$ @ 5 Hz, was also positioned in the Helmholtz coils to act as a calibration source.

A plot of the response of the xylophone magnetometer, as a function of magnetic field (as measured by the adjacent fluxgate magnetometer) over the range of ±40 nT, is shown in Fig. 4. The superimposed line is a linear fit to the data. The response is given in arbitrary units since it represents the output of the lock-in amplifier. It is apparent from these results that the

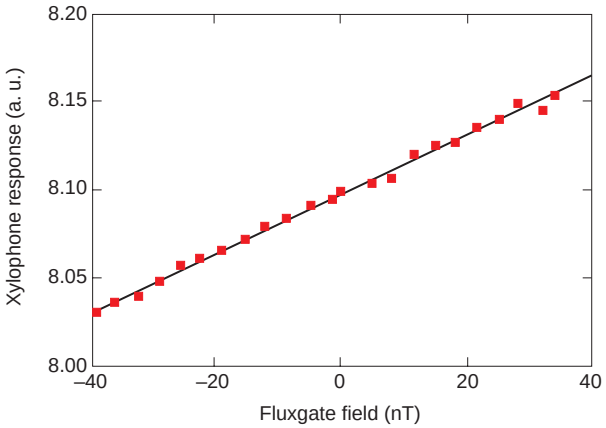

Figure 4. Output response of the xylophone magnetometer, in arbitrary units, as a function of magnetic field (measured by the fluxgate magnetometer) over the range ±40 nT.

response of the xylophone device is linear over this range and that its sensitivity is at least 1 nT and probably at least equal to that of the fluxgate magnetometer. This action is even more dramatically illustrated in Fig. 5, which depicts the fields measured by the two magnetometers during the course of a data collection run. The short-range variations in signal levels of the two magnetometers track to a remarkable extent and are the result of small temporal variations in the local magnetic field, including those caused by the motion of magnetic objects in adjacent areas. These variations are also thought to cause the majority of the scatter observed in Fig. 4. The fine detail in Fig. 5 is more pronounced for the xylophone trace, hinting at perhaps higher sensitivity and/or faster speed of response, although it is not known how much the output of the fluxgate has been smoothed by filtering. The similarity in signals of the two devices also points out that since no particular care was taken to mechanically isolate the setup, normal vibrations, away from the fundamental resonance frequency, do not appear to be a serious interference source for the xylophone resonator. The true sensitivity and noise floor of the device can only be determined by repeating the measurements in a vibration-free environment with adequate magnetic shielding.

An indication of the increased range of the xylophone magnetometer is obtained by ramping the current through the Helmholtz coils at an approximately linear rate and generating magnetic fields over the range ±0.8 mT. The results are given in Fig. 6 and demonstrate that the device remains linear over this complete range, a range limited only by the current-carrying capacity of the Helmholtz coils (20 A). For comparison purposes, the range of operation of the fluxgate magnetometer is also indicated. Note that the fluxgate range of ±0.1 mT is not zero-centered because of residual background fields in the laboratory.

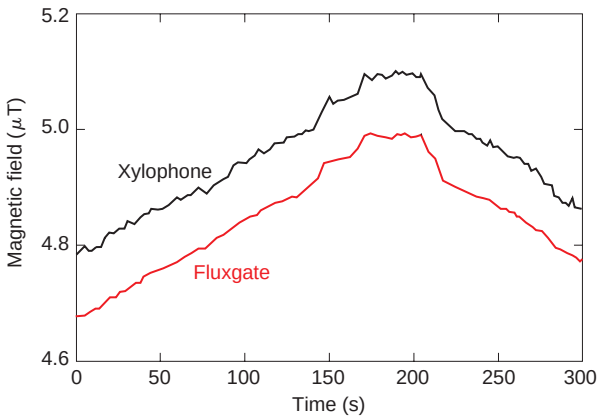

Figure 5. Comparison of the temporal variation in output responses of the xylophone and the fluxgate magnetometers. The response of the xylophone magnetometer has been offset by 0.1 μT for clarity.

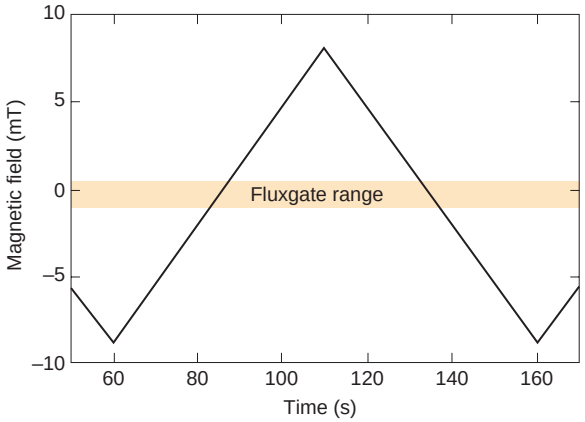

Figure 6. Measurement with the xylophone magnetometer in the range of ±8 mT, obtained by an approximately linear ramp between ±20 A in the Helmholtz coils.

The high sensitivity of the xylophone magnetometer is partly due to the high Q-factor of the structure. For example, the Q of a 39.00 × 5.17 × 0.9 mm resonator under ambient conditions was 1220. This increased to only 1305 when operated in a helium atmosphere, indicating that little damping was occurring due to viscous drag. The sensitivity can be increased still further by increasing the resonance-drive current beyond the present 1 A. The resistance of the device is on the order of 1 mΩ and can be reduced still further by optimization of the wire-bonding process. The power dissipation, which is on the order of a few milliwatts, does not introduce any significant thermal problems. In a similar manner, the operating range of the device can be substantially increased by reducing the resonance drive current. The sensitivity is directly proportional to the drive current and, for example, decreasing this to 1 mA will increase the range of operation to at least 1 T. For a given drive current, the instantaneous dynamic range exceeds 10^4 or 80 dB, a level set by the signal processing electronics used.

FUTURE TRENDS

At present, the maximum bandwidth of the xylophone structure (f_0 = 2.79 kHz; $Q \approx 1200$) is only a few hertz. This bandwidth can be increased by positioning the nodal supports appropriately and driving the resonator at an overtone frequency. Alternatively, the fundamental frequency can be increased significantly by decreasing the dimensions of the structure since it is inversely proportional to the square of the length. The dimensions of the prototype device were chosen arbitrarily (and determined largely by dexterity in operating a metal shear). Several additional advantages will accrue in going to smaller structures. First, when monitoring AC magnetic fields, the contribution of the *1/f* noise will be reduced. Second, it should be readily possible to fabricate the resonators, together with in-

tegral supports, using conventional photolithography and/or MEMS- or LIGA-processing (German acronym for LIthographie, Galvanoformung, Abformung) techniques.[12] Third, the availability of micromachined components will permit the development of compact, fully integrated systems using, for example, capacitive detection and standard signal processing. There may be some disadvantages in going to smaller sizes, particularly in reduced signal intensities, but these will be quantified as the technology develops. Finally, it will become possible to fabricate arrays of sensors to allow for high-sensitivity magnetic imaging.

As an example of what is possible with MEMS processing, Fig. 7 shows an APL-conceived three-axis magnetometer on a planar chip with side dimensions that could be in the range of less than 2 to 10 mm. In a true integration of miniature magnetometer technology, B_x is measured by a magnetostrictive cantilever, B_y by a xylophone resonator, and B_z by a magnetic moment diaphragm. The latter consists of a hard magnetic film deposited on one side of a diaphragm, which rotates about the central torsion arm in response to the component of the field vector normal to the plane of the diagram. The chip can be fabricated at the MUMPs foundry at MCNC with APL processing limited to the selective deposition of the magnetostrictive and hard magnetic films on the cantilever and diaphragm, respectively. An SEM photograph of an MCNC-processed miniature xylophone resonator is shown in Fig. 8. The deflections of the three vector components will be sensed capacitively, and it is envisioned that the necessary signal processing circuitry will be mounted on or close to the magnetometer chip to minimize stray capacitances. Finally, it is equally feasible to develop linear or area arrays of these different types of magnetometer to meet other possible applications. The applicability of any one type to any particular use will depend on the physical and electrical specifications. For example, current work is being carried out under a collaborative Independent Research and Development project with the APL Space Department partly to determine which class of magnetometer can be used to produce flight-qualified devices.

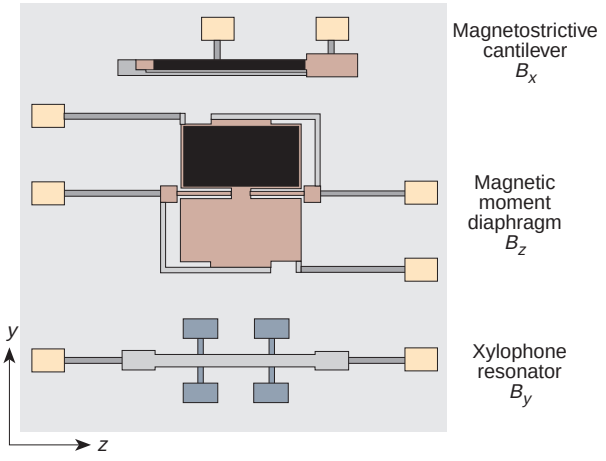

Figure 7. A miniature three-axis vector magnetometer based on a magnetostrictive cantilever B_x, a xylophone resonator B_y, and a magnetic moment diaphragm B_z. The active magnetic coatings (black) will be selectively deposited at APL.

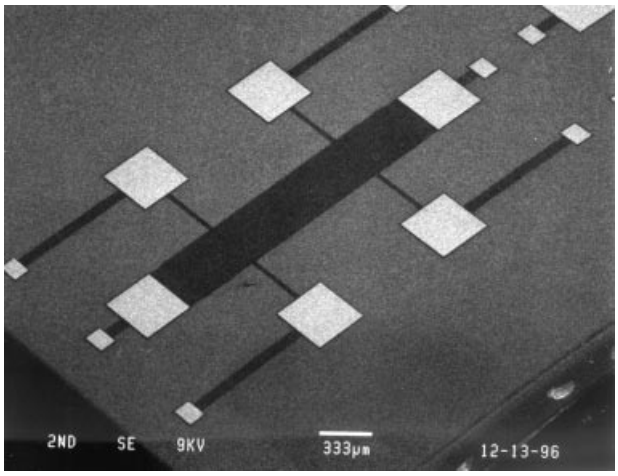

Figure 8. SEM photograph of an MCNC-processed miniature xylophone resonator.

SUMMARY

Two different types of novel magnetometers have been devised and developed within the Sensor Science Group of APL's Milton S. Eisenhower Research and Technology Development Center. The first uses, as an active element, a commercial (001) silicon microcantilever coated with an amorphous thin film of the giant magnetostrictive alloy Terfenol-D and a compact optical beam deflection transduction scheme. It has been demonstrated with a sensitivity near 1 μT. The second is a conceptually simpler Lorentz-force magnetometer based on a classical xylophone resonator and a larger bench-top optical beam transduction scheme. It has been shown to have a sensitivity of at least 1 nT, comparable to that of a commercial fluxgate magnetometer, and a dynamic range exceeding 80 dB. Both classes of magnetometer, even though at an early stage of development, offer a number of advantages for field applications: small size, high sensitivity, integration on a silicon chip, and vector capability. Both classes, together with others, can be fabricated using standard MEMS processing techniques into planar three-axis magnetometers and into one- or two-dimensional arrays for magnetic imaging applications. These magnetometers currently are a few orders of magnitude away from that required in typical interplanetary measurements, but are quite suitable, even at their present state of technological development, for attitude determination and self-noise cancellation roles in space applications.

REFERENCES

[1]Lenz, J. E., "A Review of Magnetic Sensors," *Proc. IEEE* **78**, 973–989 (1990).
[2]Rossel, C., Bauer, P., Zech, D., Hofer, J., Willemin, M., and Keller, H., "Active Microlevers as Miniature Torque Magnetometers," *J. Appl. Phys.* **79**, 8166–8172 (1996).
[3]Miller, L. M., Podosek, J. A., Kruglick, E., Kenny, T. W., Kovacich, J.A., and Kaiser, W. J., "A μ-Magnetometer Based on Electron Tunneling," *Proc. IEEE Workshop on Microelectromech. Sys.*, IEEE, New York, pp. 467–472 (1996).
[4]Clark, A. E., in *Ferromagnetic Materials*, E. P. Wohlfahrt (ed.), North-Holland, Amsterdam, p. 531 (1980).
[5]Greenough, R. D., Schultz, M. P., Jenner, A. G. I., and Wilkinson, A. J., "Actuation with Terfenol-D," *IEEE Trans. Magn.* **27**, 5346–5348 (1991).
[6]Vranish, J. M., Naik, D. P., Resteroff, J. B., and Teter, J. P., "Magnetostrictive Direct Drive Rotary Motor Development," *IEEE Trans. Magn.* **27**, 5355–5357 (1991).
[7]Chung, R., Weber, R., and Jiles, D. C., "A Terfenol-Based Magnetostrictive Diode Laser Magnetometer," *IEEE Trans. Magn.* **27**, 5358–5360 (1991).
[8]Mermelstein, M. D., and Dandridge, A., "Low-Frequency Magnetic Field Detection with a Magnetostrictive Amorphous Metal Ribbon," *Appl. Phys. Lett.* **51**, 545–547 (1987).
[9]Honda, T., Arai, K. I., and Yamaguchi, M., "Fabrication of Magnetostrictive Actuators Using Rare-Earth (Tb,Sm)-Fe Thin Films," *J. Appl. Phys.* **76**, 6994–6999 (1994).
[10]Quandt, E., Gerlach, B., and Seeman, K., "Preparation and Application of Magnetostrictive Thin Films," *J. Appl. Phys.* **76**, 7000–7002 (1994).
[11]Schatz, F., Hirscher, M., Schnell, M., Flik, G., and Kronmuller, H., "Magnetic Anisotropy and Giant Magnetostriction of Amorphous TbDyFe Films," *J. Appl. Phys.* **76**, 5380–5382 (1994).
[12]Benson, R. C., Murphy, J. C., and Charles, H. K., Jr., "Miniature Sensors Based on Microelectromechanical Systems," *Johns Hopkins APL Tech. Dig.* **16** (3), 311–318 (1995).
[13]Osiander, R., Ecelberger, S. A., Givens, R. B., Wickenden, D. K., Murphy, J. C., and Kistenmacher, T. J. "A Microelectromechanical-Based Magnetostrictive Magnetometer," *Appl. Phys. Lett.* **69**, 2930–2931 (1996).
[14]Givens, R. B., Murphy, J. C., Osiander, R., Kistenmacher, T. J., and Wickenden, D. K., "A High Sensitivity, Wide Dynamic Range Magnetometer Designed on a Xylophone Resonator," *Appl. Phys. Lett.* **69**, 2755–2757 (1996).
[15]Young, W. C., *Roark's Formulas for Stress & Strain*, 6th Ed., McGraw-Hill, New York (1989).

ACKNOWLEDGMENTS: We would like to thank our colleagues in the Space Department, and Lawrence J. Zanetti, David A. Lohr, Thomas A. Potemra, and Robert E. Jenkins in particular, for their encouragement and support.

THE AUTHORS

DENNIS K. WICKENDEN is a physicist in the Sensor Science Group of the Milton S. Eisenhower Research and Technology Development Center at APL. He received his B.Sc. and Ph.D. in physics from the Imperial College of Science and Technology (University of London) in 1962 and 1965, respectively. After a postdoctoral fellowship at the University of Notre Dame, he was employed at the GEC Hirst Research Centre in England on the growth, characterization, and application of a variety of compound semiconductors, including gallium nitride, zinc sulfide, and gallium arsenide. In 1985, he moved to Portland, Oregon, to serve as Senior Scientist at Crystal Specialties, developing epitaxial growth equipment for the semiconductor industry. In 1987, he joined APL as a Senior Staff physicist. His current research interests include growth and characterization of gallium nitride and related alloys and the development of micro-electromechanical sensors. He was elected a Fellow of the Institute of Physics in 1973. His e-mail address is Dennis.Wickenden@jhuapl.edu.

THOMAS J. KISTENMACHER is a Principal Professional Staff chemist in the Milton S. Eisenhower Research and Technology Development Center at APL. He obtained a B.S. in chemistry from Iowa State University, and an M.S. and a Ph.D., also in chemistry, from the University of Illinois. During 1969-71, he was a junior fellow in the A. A. Noyes Laboratory for Chemical Physics at the California Institute of Technology. From 1971 to 1982, he served on the faculties of The Johns Hopkins University and the California Institute of Technology. Dr. Kistenmacher joined APL in 1982 as a member of the Microwave Physics Group. He subsequently served in the Materials Science Group and is currently a member of the Sensor Science Group. His principal research interests include the fabrication and analysis of thin films for a variety of structural, electronic, magnetic, and optical applications; X-ray diffraction; and crystalline structure and structure–property relationships in a variety of electronic and magnetic materials. His e-mail address is Thomas.Kistenmacher@jhuapl.edu.

ROBERT OSIANDER is a physicist in the Sensor Science Group of the Milton S. Eisenhower Research and Technology Development Center at APL. He earned an M.S and a Ph.D., both in physics, in 1986 and 1991, respectively, from the Technische Universität München in Munich, Germany, where he worked on thermal wave spectroscopy. He joined the Materials Science Group at APL as a postdoctoral fellow in 1991, and he became a member of the Senior Professional Staff in 1995 as a member of the Sensor Science Group. His current research interests include the development of microwave and thermographic techniques for nondestructive evaluation and materials' characterization, high-resolution microwave imaging, development and testing of microelectromechanical sensors, electromagnetic interaction with biological systems, and medical applications of thermographic methods. His e-mail address is Robert.Osiander@jhuapl.edu.

SCOTT A. ECELBERGER is an engineer in the Sensor Science Group of the Milton S. Eisenhower Research and Technology Development Center at APL. He received a B.S. in physics from the Pennsylvania State University in 1986 and an M.S. in applied physics from The Johns Hopkins University in 1995. He joined APL in 1987 after working as an engineer for radio stations WCED and WOWQ. As a member of the Materials Science Group, he developed techniques for the deposition and characterization of a range of metals and semiconductor compounds. Since the formation of the Sensor Science Group in 1994, he has been involved in MEMS-based sensors, surface acoustic wave devices, and time-of-flight mass spectrometry. His e-mail address is Scott.Ecelberger@jhuapl.edu.

R. BEN GIVENS is an Associate Staff member of the Sensor Science Group of the Milton S. Eisenhower Research and Technology Development Center at APL. He studied electronics while in the U.S. Army and later obtained an associate's degree in electronics from the Capitol Radio Engineering Institute. He joined APL in 1985 after working for the Maryland Electronic Manufacturing Company, where he focused primarily on evaluating instrument landing systems. Mr. Givens is the inventor of the Lorentz-force magnetometer described in this article. His e-mail address is Robert.Givens@jhuapl.edu.

JOHN C. MURPHY is a physicist and supervisor of the Sensor Science Group of the Milton S. Eisenhower Research and Technology Development Center at APL. He received a B.A. from The Catholic University of America in 1957, an M.S. from Notre Dame University in 1959, and a Ph.D. from Catholic University in 1970. His work includes research and development of counterfeit deterrence features in U.S. currency, and the development and applications of thermal imaging, including infrared thermography. He currently holds a part-time appointment in the Department of Biomedical Engineering of The Johns Hopkins University. Dr. Murphy chairs the APL Graduate Fellowship Committee and is a member of the Executive Committee of the Johns Hopkins Center for Nondestructive Evaluation. His e-mail address is John.Murphy@jhuapl.edu.